

## Gamma-emitting states in $^{22}\text{Ne}$

C. Broude,\* W. G. Davies, J. S. Forster, and G. C. Ball

*Atomic Energy of Canada Limited, Physics Division, Chalk River Nuclear Laboratories, Chalk River, Ontario, Canada KOJ 1J0*

(Received 2 October 1975)

Thirty-seven  $\gamma$ -emitting levels have been observed in  $^{22}\text{Ne}$  up to an excitation energy of 11.48 MeV following the reaction  $^{19}\text{F}(\alpha, p\gamma)^{22}\text{Ne}$  at  $E_\alpha = 20.0$  MeV. The decay modes and particle- $\gamma$  correlations of 22 of these levels have been measured. Seven levels of spin 5 or greater have been observed above 8.7 MeV excitation. Extensive collective band structure consistent with the available experimental evidence is proposed.

[NUCLEAR REACTIONS  $^{19}\text{F}(\alpha, p\gamma)$ ,  $E = 20.0$  MeV; measured  $\sigma(E_p, E_\gamma, \theta_\gamma, \theta_{p\gamma})$ .  $^{22}\text{Ne}$  deduced levels,  $\gamma$ -branching ratios,  $J$ ,  $\gamma$ -mixing ratios. Natural target.]

### I. INTRODUCTION

The nucleus  $^{22}\text{Ne}$  lies between two nuclei,  $^{20}\text{Ne}$  and  $^{24}\text{Mg}$ , which have been shown to have very well defined collective energy-band structure. In mass 22 nuclei much information has been obtained<sup>1</sup> for rotational structure of  $T=0$  levels in  $^{22}\text{Na}$ . Little is known, however, about rotational bands with  $T=1$  in mass 22. For  $^{22}\text{Na}$  definite spins of only the  $0^+$  and  $2^+$  have been established<sup>1</sup> with a candidate for the  $4^+$  member of the  $T=1$  ground state band. In  $^{22}\text{Mg}$  the  $0^+$ ,  $2^+$ , and  $4^+$  members of the ground band have been determined<sup>2</sup> and a candidate for the  $6^+$  level suggested.

From a purely experimental point of view, there is no easily accessible heavy ion reaction for producing  $^{22}\text{Ne}$  such as the  $^{12}\text{C}(^{12}\text{C}, \alpha)^{20}\text{Ne}$  and  $^{12}\text{C}(^{16}\text{O}, \alpha)^{24}\text{Mg}$  reactions which preferentially populate states of high angular momentum in a way ideally suited to the most commonly applied method of  $\gamma$ -ray angular correlations, method II of Litherland and Ferguson.<sup>3</sup> This type of reaction, involving all zero spins, has yielded a great deal of information about the spin and parity of levels in  $^{20}\text{Ne}$  and  $^{24}\text{Mg}$ .

In  $^{22}\text{Ne}$ , by contrast, most  $\gamma$ -ray measurements<sup>4,5</sup> have been made following the reactions  $^{19}\text{F}(\alpha, p)^{22}\text{Ne}$  and  $^{20}\text{Ne}(t, p)^{22}\text{Ne}$ , which are not ideally suited to the axially symmetric type of correlation measurement, as they allow magnetic substate populations of 0 and 1. Information on the parity of states cannot be obtained from this reaction. Some additional information about the spin and parity of levels in  $^{22}\text{Ne}$  has been obtained from the  $^{22}\text{Ne}(\alpha, \alpha')^6$  reaction and also from the heavy ion reaction  $^{14}\text{C}(^{12}\text{C}, \alpha)^{22}\text{Ne}$ ,<sup>7</sup> but the latter requires a difficult radioactive target and the yield has been found to be low compared with reactions on the residual natural  $^{12}\text{C}$ .

In previous  $\gamma$ -ray studies<sup>4,5</sup> levels were excited up to about 7 MeV only. The purpose of the pres-

ent experiment was to extend this with the aim of locating a possible  $8^+$  state belonging to the ground state rotational band predicted to lie at about 11 MeV.<sup>8</sup> Candidates for this state were found and reported briefly in a previous publication.<sup>9</sup> The present description includes a reanalysis of the data included in that reference, and supersedes it. The present paper gives results of particle- $\gamma$  angular correlation measurements on 22  $\gamma$ -emitting states in  $^{22}\text{Ne}$  up to 11.5 MeV and allows tentative classification of a number of levels into feasible collective bands based on the ground and excited states.

### II. EXPERIMENTAL PROCEDURE

A 50 nA beam of 20.0 MeV  $^4\text{He}^{++}$  ions from the Chalk River MP tandem bombarded a target of  $100 \mu\text{g}/\text{cm}^2$   $^6\text{LiF}$  evaporated onto a  $10 \mu\text{g}/\text{cm}^2$  carbon foil; the target was electrically suppressed to trap secondary electrons. The beam passed through an annular Si surface barrier particle detector which subtended an angle from  $172^\circ$  to  $177^\circ$  with respect to the beam; the particle detector, which was 1 mm thick, was covered with a  $200 \mu\text{g}/\text{cm}^2$  aluminum foil to eliminate light from the target. The detector was also cooled to about  $-25^\circ\text{C}$  by connecting it to a cold finger which passed through the vacuum chamber and dipped into liquid nitrogen; this cooling reduced the leakage current in the detector by about a factor of 10 and made it possible to operate with rates of  $\sim 10^4$  particles per second with an over-all resolution for the reaction protons of 50 keV. Figure 1 shows the particle spectrum in coincidence with any  $\gamma$  ray.

The beam was collected in a 3 m long Faraday cup, the end of which was heavily shielded to prevent  $\gamma$  radiation from reaching the NaI detectors.

Six 12.5 cm diam  $\times$  15.0 cm long NaI(Tl) detectors, each surrounded by a 2.5 cm thick lead

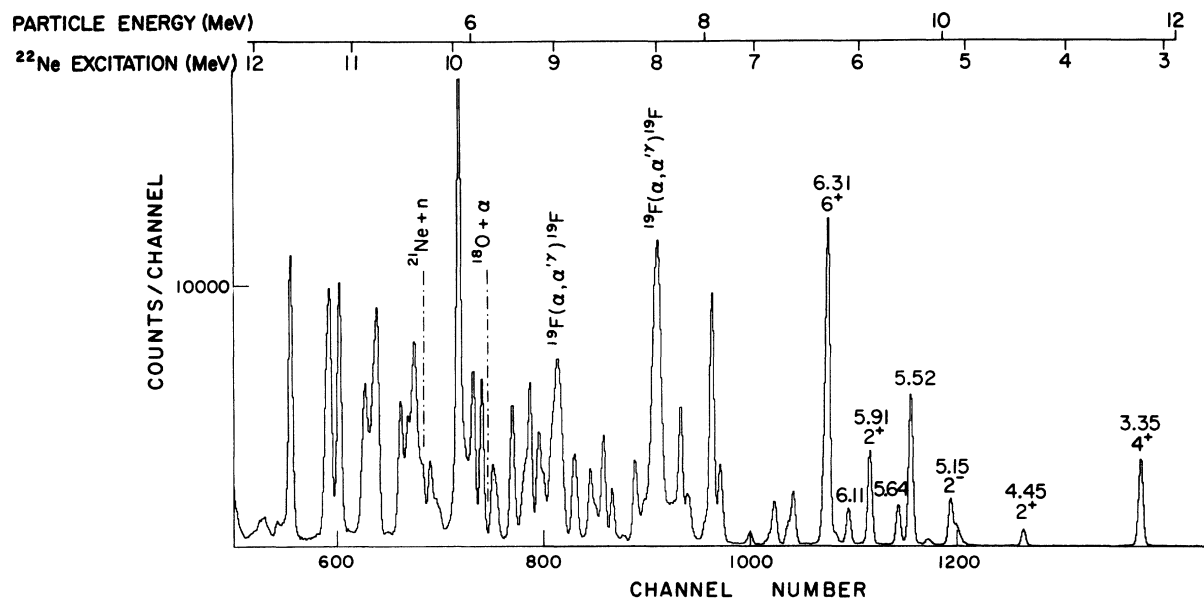


FIG. 1. Particle energy spectrum from the bombardment of a  $^6\text{LiF}$  target by 20.0 MeV  $\alpha$  particles, in coincidence with any of the six NaI(Tl) detectors of the Lotus goniometer.

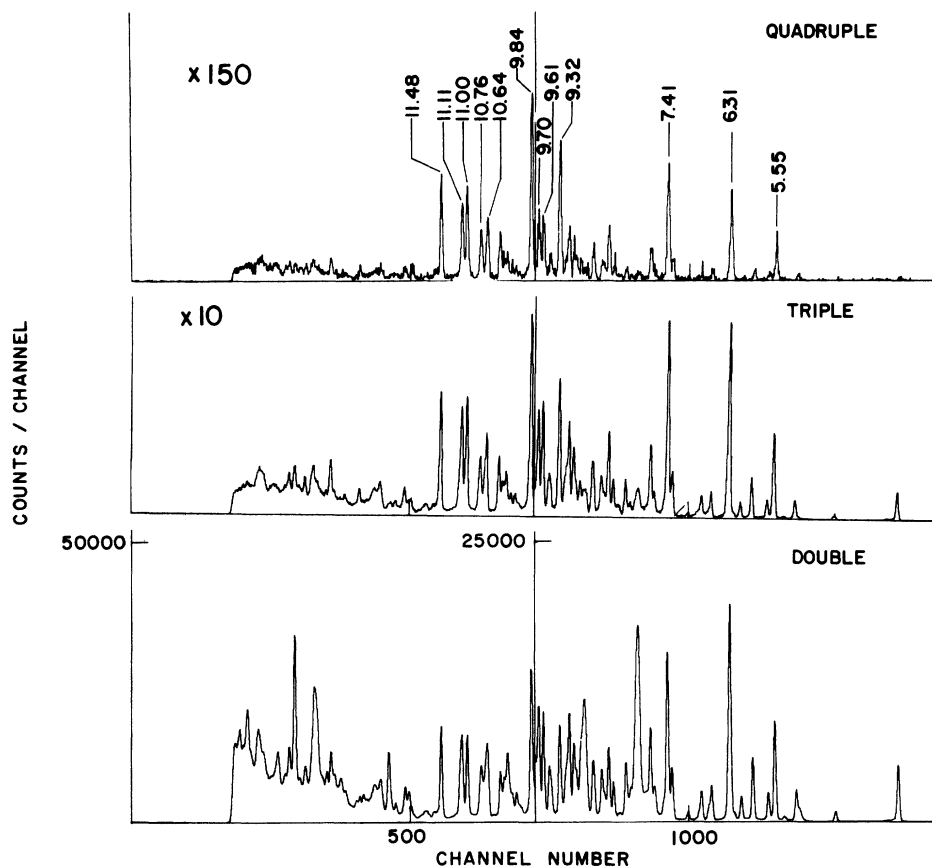


FIG. 2. Particle energy spectra with the requirement of one coincident  $\gamma$  ray (bottom), two coincident  $\gamma$  rays (center), and three coincident  $\gamma$  rays (top).

shield and coupled to a Philips XP1040 phototube, were mounted on the Chalk River LOTUS multiarm  $\gamma$ -ray goniometer.<sup>10</sup> The front face of each crystal was 18.0 cm from the target. The detectors were distributed in declination and azimuth, forward and backward of  $90^\circ$ , to produce effective angles  $\theta$  that were approximately uniformly spaced in  $\cos^2(\theta)$  from 0.0 to 0.74, the maximum being determined by the closest approach of the detectors to the beam tube.

Coincidences between the particle detector and each of the NaI(Tl) detectors were obtained with six independent TAC's (time-to-amplitude converters). The analog outputs of these TAC's were summed and fed into an ADC (analog-to-digital converter). A logical output from this summed coincidence requirement was also fed into the slow coincidence channel derived from the linear outputs of the particle- and  $\gamma$ -ray detectors and produced gating signals for seven other ADC's used for digitizing the energy information from the particle and six  $\gamma$ -ray detectors. The multiparameter information from this system was accumulated by a PDP-1 on-line computer which, in addition to producing on-line spectra from all detectors and the TAC's for monitoring, also recorded all of the event-by-event data on magnetic tape for later sorting off line by a PDP-10 computer.

Summation of the TAC analog signals had advantages other than requiring just one ADC for this channel. It was arranged to give separate time peaks for different multiplicities of  $\gamma$  rays involved in each event. Thus it was possible to set time and random background windows separately on the peaks corresponding to double, triple, and quadruple coincidences (i.e., particle plus 1, 2, or 3 coincident  $\gamma$  rays). The large number of  $\gamma$  detectors (6) plus the occurrence of many  $\gamma$ -ray cascades involving three or more transitions resulted in a significant number of these high order coincidence events.

### III. ANALYSIS

The event-recorded data were sorted by a PDP-10 computer. The initial sort located the positions of the one-, two-, and three- $\gamma$  peaks in the time spectra and suitable regions for random coincidence estimation. All further playbacks used these time windows which correspond to the full particle- and  $\gamma$ -energy ranges. Next, particle spectra were sorted in coincidence with each of the three time windows separately with no restrictions on the  $\gamma$ -ray energies. These spectra are shown in Fig. 2; an expanded version of the particle spectrum in coincidence with singles  $\gamma$  rays is shown in Fig. 1. Peaks from the  $^{19}\text{F}(\alpha, \alpha')^{19}\text{F}$

TABLE I. Excitation energies of  $\gamma$ -emitting states in  $^{22}\text{Ne}$ . An asterisk indicates that the  $\gamma$  decay of the level has been investigated. T indicates the level has been observed in strong coincidence with triple coincident  $\gamma$  rays. D indicates doubly coincident  $\gamma$  rays; no symbol indicates coincidence with a single  $\gamma$  ray.

| Level no. <sup>c</sup> |    | $E_x$ <sup>a</sup><br>present work<br>(MeV) | $\Delta E$ <sup>b</sup><br>(keV) |
|------------------------|----|---|----------------------------------|
| 2                      | D  | 3.383                                       | 27                               |
| 3                      |    | 4.466                                       | 9                                |
| 4                      | D  | 5.148                                       | 4                                |
| 7                      | *D | 5.523 <sup>d</sup>                          | 2                                |
| 8                      | *D | 5.641                                       | 4                                |
| 9                      | *D | 5.907                                       | -7                               |
| 10                     | *D | 6.108                                       | -8                               |
| 12                     | *T | 6.308                                       | +8                               |
| 14                     | D  | 6.631                                       | -13                              |
| 16                     | *D | 6.809                                       | -10                              |
| 19                     | *  | 7.042                                       | -10                              |
| 20                     | *D | 7.314                                       | -22                              |
| 23                     | *T | 7.406                                       | -34                              |
| 27                     | D  | 7.618                                       | -14                              |
| 29                     | *D | 7.704                                       | -17                              |
| 32                     | *  | 8.139                                       | +3                               |
| 33                     | *  | 8.353                                       | -28                              |
| 34                     | *D | 8.441                                       | -58                              |
| 36                     | D  | 8.563                                       | -12                              |
| 37                     | *D | 8.716                                       | -8                               |
| 40                     | D  | 8.941                                       | -29                              |
| 42                     | D  | 9.053                                       | -16                              |
| 43                     | D  | 9.150                                       | -24                              |
| 46                     | T  | 9.317                                       | +1                               |
| 48                     |    | 9.485                                       |                                  |
| 49                     | *D | 9.609                                       |                                  |
| 50                     | D  | 9.697                                       |                                  |
| 51                     | T  | 9.838                                       |                                  |
| 52                     | D  | 10.105                                      |                                  |
| 53                     | D  | 10.183                                      |                                  |
| 54                     | D  | 10.269                                      |                                  |
| 55                     | *T | 10.405                                      |                                  |
| 56                     | *T | 10.634                                      |                                  |
| 57                     | *T | 10.755                                      |                                  |
| 58                     | *T | 11.000                                      |                                  |
| 59                     | *T | 11.102                                      |                                  |
| 60                     | *T | 11.482 <sup>d</sup>                         |                                  |

<sup>a</sup> Errors in the quoted energies are  $\pm 20$  keV absolute.

<sup>b</sup> The  $\Delta E$  quoted are the differences between the excitation energies of Ref. 18 and the present values except for the 6.31 MeV level which is compared to Ref. 13.

<sup>c</sup> Level numbering is taken from Ref. 18, up to level 46.

<sup>d</sup> The calibration energies are the result of Ge(Li) detector measurements, level 7 from Ref. 12, level 60 from Ref. 13.

reaction are easily identified by their larger width resulting from the larger kinematic broadening in this reaction. In some cases proton and  $\alpha$  peaks coincide and then the multiple- $\gamma$ -ray particle spectra have helped in assigning optimum windows for playback of  $\gamma$  rays in coincidence with the  $^{22}\text{Ne}$  groups. An example of this is the proton group to the 11.11 MeV level which appears broader than its two neighbor peaks in the bottom spectrum of Fig. 2. This peak becomes narrower, in coincidence with two and three  $\gamma$  rays as an  $^{19}\text{F}$  contaminant

peak is eliminated. Another example is the improvement in the separation of the 10.64 and 10.76 MeV excitation peaks as shown in Fig. 2.

The excitation energies from the three spectra of Fig. 2 were determined automatically by a peak finding algorithm<sup>11</sup> incorporating a linear calibration derived from the accurately known  $5522.5 \pm 0.7$ <sup>12</sup> and  $11482 \pm 3$  keV<sup>13</sup> levels of  $^{22}\text{Ne}$  and an estimated mean detector angle of  $174^\circ$ . The calibration procedure included the effects of the variable energy loss from the  $200 \mu\text{g}/\text{cm}^2$  masking

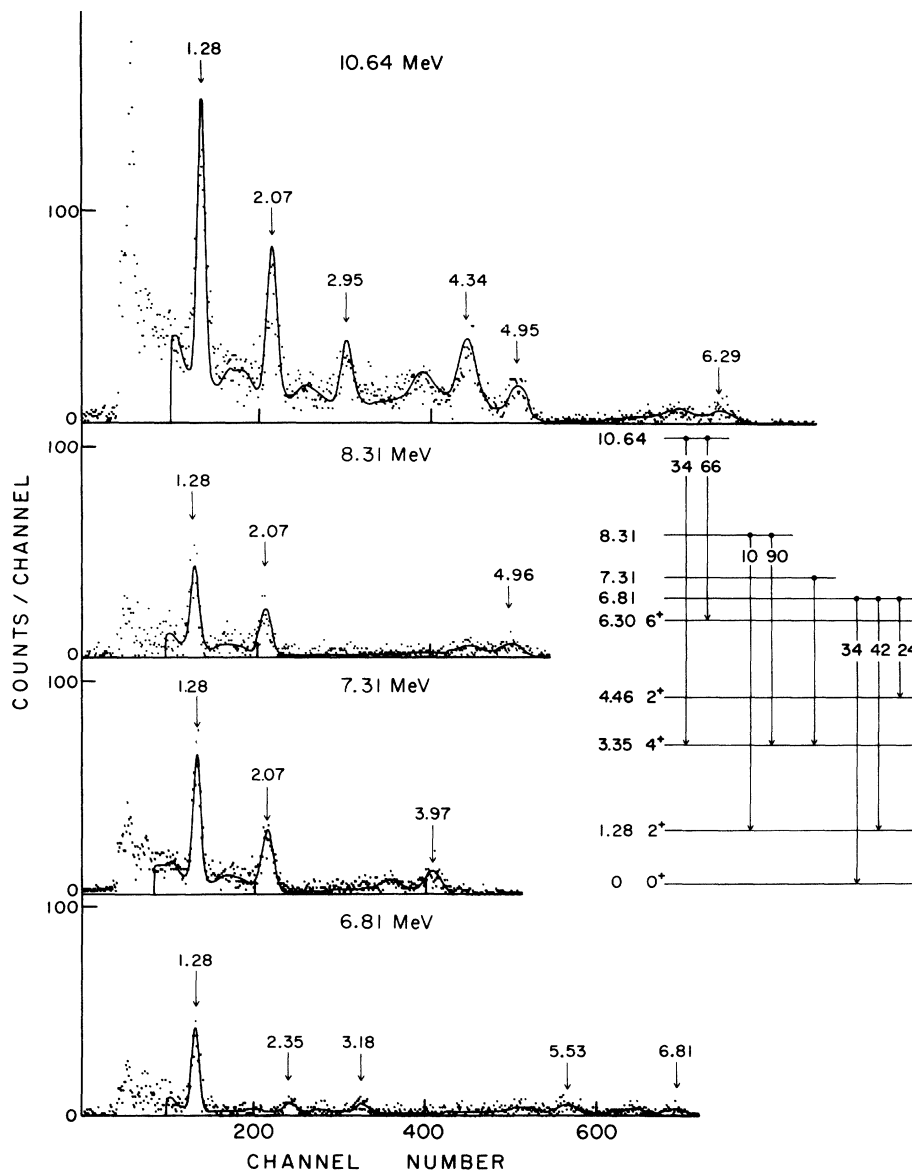


FIG. 3. Typical  $\gamma$ -ray spectra from a single 12.5 cm diam x 15 cm long NaI(Tl) detector in coincidence with the particle peaks corresponding to excitation energies in  $^{22}\text{Ne}$  of 6.81, 7.31, 8.35, and 10.64 MeV (levels numbered 16, 20, 33, and 56 in Table I). The curves through the spectra are the result of the least squares  $\gamma$ -ray fitting procedure and the observed decay schemes of the four levels are shown in the insert.

foil on the particle detector. These proton energies were then processed in a second program which calculated the excitation energies. The excitation energies resulting from the three independent particle spectra (Fig. 2) have been cross checked to give the listing in Table I. An absolute error of  $\pm 20$  keV has been assigned to these level energies though the relative energy error is about  $\pm 5$  MeV.

Using the established time and proton-energy windows, the data were sorted to give six separate

$\gamma$ -ray spectra for each particle group, summed over all of the three time windows and with suitable random coincidence subtraction. Coincidence events involving more than one  $\gamma$  ray were all sorted into their appropriate NaI(Tl) spectra. In this playback, 2 passes were required to sort on all 37 proton peaks. Examples of  $\gamma$  spectra are shown in Figs. 3 and 4, corresponding to the indicated proton groups.

To obtain the relative intensities of the  $\gamma$  rays in these data, all  $\gamma$ -ray spectra were fitted using

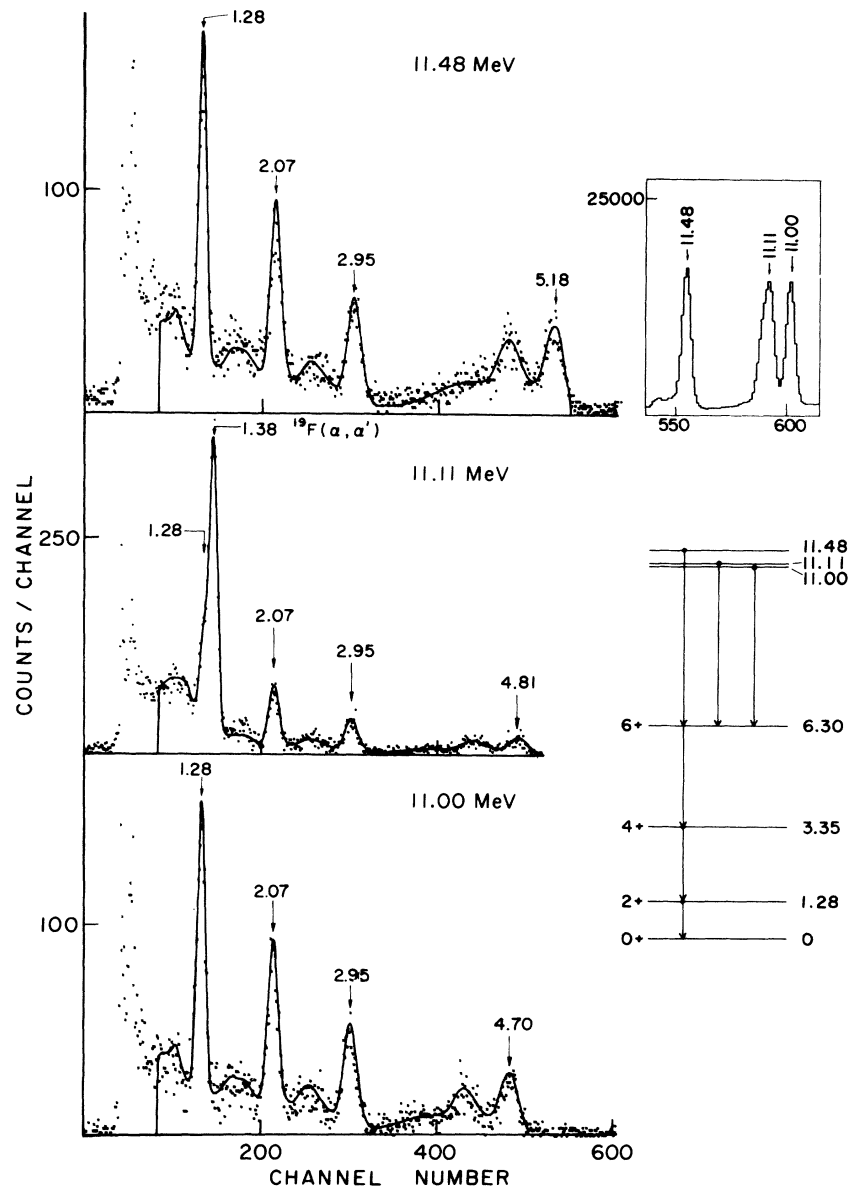


FIG. 4.  $\gamma$ -ray spectra from the 11.00, 11.11, and 11.48 MeV levels in  $^{22}\text{Ne}$ , with the least squares fit to the data. The relevant section of the particle spectrum is shown in the insert at the top right and the decay schemes at the bottom right. The 1.38 MeV  $\gamma$  ray originates from  $^{19}\text{F}(\alpha, \alpha')^{19}\text{F}$ .

TABLE II.  $\gamma$ -ray branching ratios of states in  $^{22}\text{Ne}$ . The values in parentheses are from the work of Howard *et al.* (Ref. 5). All other values are from the present experiment and have a probable error of  $\pm 5\%$ .

| Initial state |              | Final state        |                       |                       |                               |                       |                       |
|---------------|--------------|--------------------|-----------------------|-----------------------|-------------------------------|-----------------------|-----------------------|
| Level no.     | Energy (MeV) | 0(0 <sup>+</sup> ) | 1.28(2 <sup>+</sup> ) | 3.35(4 <sup>+</sup> ) | (MeV, $J^\pi$ ) branching (%) | 4.46(2 <sup>+</sup> ) | 6.30(6 <sup>+</sup> ) |
| 4             | 5.15         |                    | 53(53)                |                       | 47(47)                        |                       |                       |
| 7             | 5.52         |                    |                       | 100(100)              |                               |                       |                       |
| 8             | 5.64         |                    | 68(77)                | 32(23)                |                               |                       |                       |
| 9             | 5.91         |                    | 80(85)                | 10(5)                 | 10(10)                        |                       |                       |
| 10            | 6.11         | (14)               | 90(78)                |                       | 10(8)                         |                       |                       |
| 12            | 6.31         |                    |                       | 100(100)              |                               |                       |                       |
| 16            | 6.81         | 34                 | 42                    |                       | 24                            |                       |                       |
| 19            | 7.04         | (9)                | 100(91)               |                       |                               |                       |                       |
| 20            | 7.31         |                    |                       | 100                   |                               |                       |                       |
| 23            | 7.41         |                    |                       |                       |                               |                       | 5.52 MeV, 100%        |
| 29            | 7.70         |                    | 16                    | 23                    | 53                            |                       | 6.12 MeV, 8%          |
| 32            | 8.14         |                    | 90                    | 10                    |                               |                       |                       |
| 33            | 8.35         |                    | 10                    | 90                    |                               |                       |                       |
| 34            | 8.44         |                    |                       | 37                    |                               |                       | 63                    |
| 37            | 8.72         |                    |                       | 53                    | 47                            |                       |                       |
| 49            | 9.61         |                    |                       | 69                    |                               |                       | 31                    |
| 55            | 10.41        |                    |                       |                       |                               |                       | 100                   |
| 56            | 10.64        |                    |                       | 34                    |                               |                       | 66                    |
| 57            | 10.76        |                    |                       | 48                    |                               |                       | 52                    |
| 58            | 11.00        |                    |                       |                       |                               |                       | 100                   |
| 59            | 11.11        |                    |                       |                       |                               |                       | 100                   |
| 60            | 11.48        |                    |                       |                       |                               |                       | 100                   |

a spectrum stripping program written by Ferguson.<sup>14</sup> This program used a set of standard monoenergetic  $\gamma$ -ray lines to produce a table of coefficients that allowed the generation of the line shape for any desired  $\gamma$ -ray energy. Reference line shapes were generated independently for each of the six LOTUS NaI(Tl) detectors, using radioactive source and reaction  $\gamma$  rays of 0.51, 0.90, 1.28, 1.84, 4.43, 6.13, and 7.12 MeV. With the shape coefficients available, the  $\gamma$ -ray spectra were individually fitted, each in terms of its own line shapes and its own energy calibration. The program required first approximations to the energy of each of the  $\gamma$  rays included in the fit; these were found by inspection. The stripping program found the energy and intensity with their standard deviations for each component  $\gamma$  ray by using a nonlinear least squares algorithm. The intensities in principle require correction for two factors: (1) the recoil velocity of the compound nucleus which produces a significant variation in efficiency of the detectors and introduces a straightforward  $2v \cos \theta / c$  correction; (2) the inherent anisotropy of the system, which was measured by using isotropic radiation at the center of the target chamber. The latter was less than 2% and was ignored.

The energies and corrected intensities were then arranged into decay schemes (see Table II);

the six intensities for each  $\gamma$ -ray transition were fitted to a Legendre polynomial series (order 0, 2, and 4) and the coefficient of the  $P_0(\cos \theta)$  term was corrected for the energy dependent detector efficiency to give relative intensities. These intensities yielded the branching ratios quoted in Table II.

Decays involving the 6.31 MeV 6<sup>+</sup> level could not be resolved from the nearby 6.35 MeV state; wherever a transition to the 6<sup>+</sup> level is assigned it is based on independent measurements with the  $^{19}\text{F}(\alpha, p\gamma)^{22}\text{Ne}$  reaction using a Ge(Li) detector in coincidence with backscattered protons.<sup>13</sup> The spin of the 6.31 MeV state has recently been confirmed in an independent experiment by Fifield, Zurmühle, and Balamuth.<sup>15</sup>

The angular correlations were analyzed using a computer program capable of simultaneously fitting arbitrary sets of parallel  $\gamma$ -ray cascades in terms of the population parameters of the initial state, the spins of all relevant levels, and the multipole mixing ratios of all mixed transitions. The magnetic substates involved can be specified and, because the fitting algorithm used quadratic programming,<sup>16</sup> the requirements of positive populations and normalization constants were built into the procedure. Magnetic substates of 0 and 1, consistent with the spins of the reaction and the

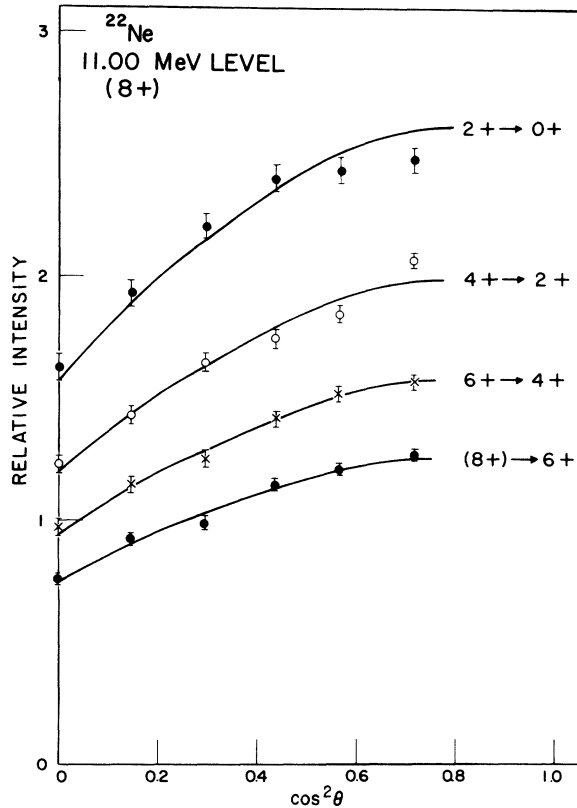


FIG. 5. The measured angular correlations for the four cascade  $\gamma$  rays from the 11.00 MeV level in  $^{22}\text{Ne}$  with their simultaneous least squares fit for an initial state spin of 8.

small size of the particle detector, were allowed in all fits. Examples of best fits are shown in Figs. 5 and 6.

In each case, all primary level spins consistent with the observed branching of the level were allowed in fitting the correlations. The following fitting procedure was adopted to ensure finding all minima as a function of the mixing ratios. In cases where no mixing ratio was involved, the quadratic programming algorithm reduces to linear programming and so the best fit was easily found. Where a single mixing ratio  $\delta$  occurred, a grid of 37 steps in the mixing was first evaluated at  $5^\circ$  intervals in  $\tan^{-1}(\delta)$ . At each value of  $\delta$ , the best fit was found with all other parameters unrestricted. A complete quadratic programming fit was then performed at each  $\chi^2$  minimum found in the grid search. In cases involving two mixing ratios, a  $37 \times 37$  grid of  $\chi^2$  versus  $\delta_1$  and  $\delta_2$  was evaluated followed by a search for all minima and execution of a full quadratic fit at each of these minima, usually four (see below) in number. An example of these fits can be seen in Fig. 7. In these cases,

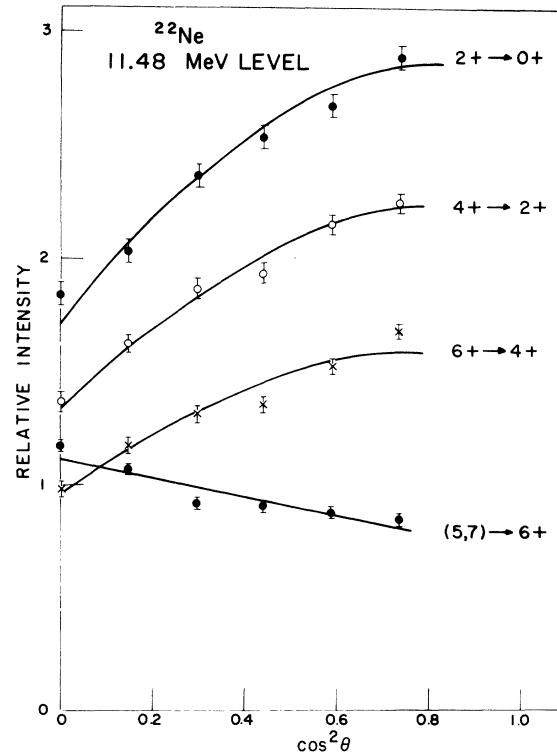


FIG. 6. The measured angular correlations for the four cascade  $\gamma$  rays from the 11.48 MeV level in  $^{22}\text{Ne}$  with their simultaneous least squares fit for the initial spins of 5 or 7.

three transitions were fitted simultaneously, i.e., from the initial 10.76 MeV state to the 6.31 MeV  $6^+$  state, from the 10.76 MeV level to the 3.35 MeV  $4^+$  state, and from the  $6^+$  state to the  $4^+$  state. The possible spin assignments 4 and 6 allow one mixed transition only and lead to the one dimensional grids shown in the bottom left of the figure. Spin 5 allows two independent mixed transitions,  $\delta_1$  and  $\delta_2$ , and leads to the contour grid plotted at upper left. Here  $\chi^2$  contours are shown on a logarithmic scale with a factor of 1.3 between adjacent contours. The four minima are clearly seen; it should be remembered that the mixing ratios are continuous in passing from  $+90^\circ$  to  $-90^\circ$ , i.e., both these values correspond to pure quadrupole radiation and so for example, the minima that appear at  $\tan^{-1}(\delta_2) = -90^\circ$  are spurious as they connect with the minima at  $\tan^{-1}(\delta_2) = +83^\circ$ . Sections passing through the minima of this plot and parallel to the  $\delta_1$  and  $\delta_2$  axes are shown in the lower left of the figure.

Errors have been assigned to the multipole mixing ratios by means of the relationship between the standard deviation of a variable and the second derivative of  $\chi^2$  with respect to that variable at

the  $\chi^2$  minimum. In cases where the value of  $\delta$  is small (less than 1), a symmetric error estimate is quoted, derived as above. When  $\delta$  is large, estimates of asymmetric confidence limits have been calculated for the inverse of the mixing ratio and then transformed back to the form of the mixing ratio which is consistently quoted in this paper, i.e., quadrupole amplitude/dipole amplitude with the sign convention used by Ferguson.<sup>17</sup>

#### IV. RESULTS

Table I lists the measured excitation energies for 37 proton groups observed in this experiment to be in coincidence with  $\gamma$  radiation.  $\alpha$  groups from inelastic scattering from  $^{19}\text{F}$ , identified by their large width and characteristic coincident  $\gamma$  rays, do not appear in the table. The excitation energies shown in Table I have been obtained as described in Sec. III and are based on calibration energies<sup>12,13</sup> of the levels at 5.523 and 11.482 MeV both derived from Ge(Li) detector  $\gamma$ -ray measurements. The observed levels have been correlated

with the listing of levels given by Endt and van der Leun<sup>18</sup> up to level 46; the level numbers appear in column 1 of Table I. In the last column are given the energy differences,  $\Delta E$  (keV), between the present excitation energies and the corresponding energies from Ref. 18. Anomalous deviations indicate levels that probably do not correspond to the nearest level quoted in Ref. 18 and may indicate new levels, for example levels numbered 20, 23, 32, 33, and 34 at 7.31, 7.41, 8.14, 8.35, and 8.44 MeV, respectively.

Appearing in Table I are the other notations: a  $T$  if the level has been seen strongly in coincidence with three discrete  $\gamma$  rays, a  $D$  if with two discrete  $\gamma$  rays, and no symbol if with only a single  $\gamma$ -ray transition. This differentiation was useful in resolving peaks that appeared as multiplets in coincidence with single  $\gamma$  rays or were obscured by  $^{19}\text{F}(\alpha, \alpha')$  lines or general background. The asterisk in Table I indicates that the  $\gamma$ -decay mode of that level has been investigated. Unmarked levels do not appear in the following results and discussion because they were either obscured by

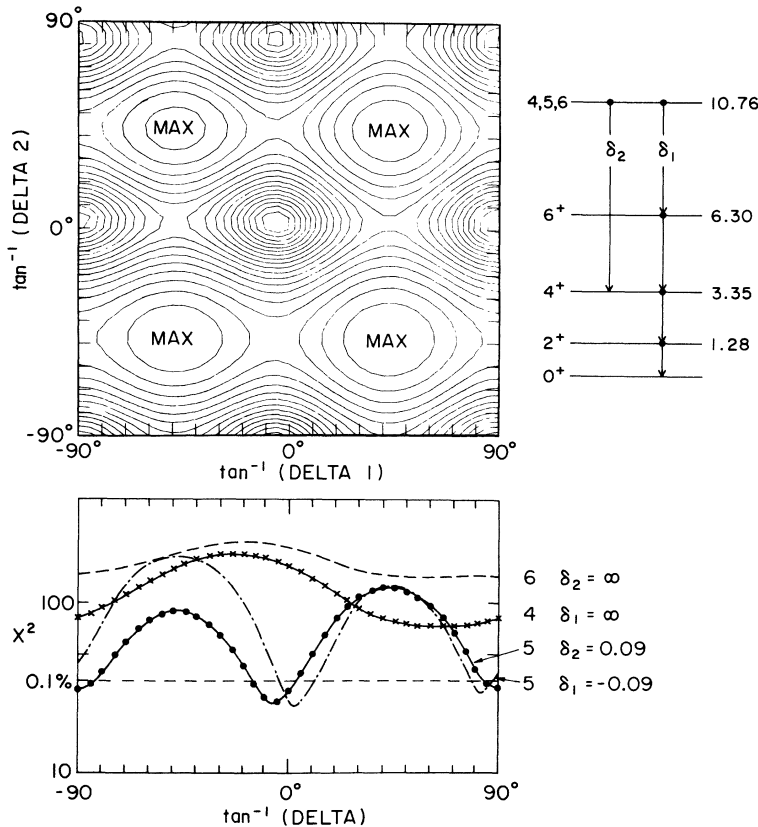


FIG. 7.  $\chi^2$  plots for the fit to the three transitions associated with the 10.76 MeV level in  $^{22}\text{Ne}$  (see the decay scheme at top right and Table III). At bottom left are shown the single multipole mixing grids for spins 4 and 6; the contour plot of the double grid for spin 5 is shown in the upper left. The two spin 5 curves in the lower left are perpendicular sections of the two-dimensional grid through its minima.



TABLE III. Correlation fitting results.

| Level<br>no. |  | Observed $\chi^2$ for spin |    |           |          |             |          |            |          | $\chi^2$ for 0.1%<br>confidence<br>limit | Degrees of<br>freedom |          |
|--------------|--|----------------------------|----|-----------|----------|-------------|----------|------------|----------|--|-----------------------|----------|
|              |  | 0                          | 1  | 2         | 3        | 4           | 5        | 6          | 7        | 8  |                       |          |
| 7            | $\rightarrow 2 \rightarrow 1 \rightarrow 0$                                |                            |    | 6         | 4        | 4           |          |            |          |  | 34                    | 13       |
| 8            | $\rightarrow 1; \rightarrow 2 \rightarrow 1$                               |                            |    | 33        | 19       | 97          |          |            |          |  | 34                    | 13       |
| 9            | $\rightarrow 1 \rightarrow 0$  | 272                        | 18 | 54        | 16       | 517         |          |            |          |  | 26                    | 8        |
| 10           | $\rightarrow 1 \rightarrow 0$  | 66                         | 10 | 7         | 14       | 61          |          |            |          |  | 28                    | 9        |
| 12           | $\rightarrow 2 \rightarrow 1$  |                            |    | 308       | 60       | 45          | 75       | 33         |          |  | 28                    | 9        |
| 16           | $\rightarrow 0; \rightarrow 1; \rightarrow 3$                              |                            | 16 | 31        |          |             |          |            |          |  | 34                    | 13       |
| 19           | $\rightarrow 1 \rightarrow 0$  | 19                         | 3  | 12        | 25       | 78          |          |            |          |  | 28                    | 9        |
| 20           | $\rightarrow 2 \rightarrow 1 \rightarrow 0$                                |                            |    | 51        | 23       | 32          | 50       | 70         |          |  | 34                    | 13       |
| 23           | $\rightarrow 7$  |                            |    | 263       | 5        | 73          | 5        | 567        |          |  | 17                    | 3        |
| 29           | $\rightarrow 1; \rightarrow 2 \rightarrow 1; \rightarrow 10 \rightarrow 1$ |                            |    | 19        | 18       | 38          |          |            |          |  | 47                    | 21       |
| 32           | $\rightarrow 1; \rightarrow 2 \rightarrow 1$                               |                            |    | 37        | 21       | 413         |          |            |          |  | 31                    | 11       |
| 33           | $\rightarrow 2 \rightarrow 1$  |                            |    | 44        | 13       | 12          |          |            |          |  | 34                    | 13       |
| 34           | $\rightarrow 2; \rightarrow 12 \rightarrow 2$                              |                            |    |           |          | 46          | 39       | 139        |          |  | 34                    | 13       |
| 37           | $\rightarrow 2 \rightarrow 1; \rightarrow 3 \rightarrow 1$                 |                            |    | {39<br>16 | 29<br>13 | 36<br>19    |          |            |          |  | 42<br>34              | 18<br>13 |
| 49           | $\rightarrow 2; \rightarrow 12 \rightarrow 2$                              |                            |    |           |          | 52          | 33       | 203        |          |  | 34                    | 13       |
| 55           | $\rightarrow 12 \rightarrow 2 \rightarrow 1$                               |                            |    |           |          | 23          | 21       | 23         | 29       | 33                                       | 34                    | 13       |
| 56           | $\rightarrow 2; \rightarrow 12 \rightarrow 2$                              |                            |    |           |          | 50          | 35       | 135        |          |  | 34                    | 13       |
| 57           | $\rightarrow 2; \rightarrow 12 \rightarrow 2$                              |                            |    |           |          | 73          | 26       | 140        |          |  | 34                    | 13       |
| 58           | $\rightarrow 12 \rightarrow 2 \rightarrow 1$                               |                            |    |           |          | 93          | 56       | 24         | 65       | 26                                       | 34                    | 13       |
| 59           | $\rightarrow 12 \rightarrow 2 \rightarrow 1$                               |                            |    |           |          | 39          | 17       | 18         | 18       | 25                                       | 34                    | 13       |
| 60           | $\rightarrow 12 \rightarrow 2 \rightarrow 1$                               |                            |    |           |          | {358<br>351 | 50<br>32 | 105<br>103 | 60<br>33 | 700<br>634                               | 42<br>34              | 18<br>13 |

background or the  $\gamma$ -ray spectra were too complex or too weak to be unraveled reliably with particle-NaI(Tl)  $\gamma$ -ray coincidence work alone.

Table II shows the measured  $\gamma$ -ray branching ratios for 22 of the observed  $^{22}\text{Ne}$  levels. The numbers in parentheses are taken from the work of Howard *et al.*<sup>5</sup> and the agreement is seen to be good. The branching ratios are normalized to 100 for each level and a probable error of  $\pm 5$  has been assigned to the measured values. It will be noted that as the excitation energy gets higher most of the observed levels decay through the 6\*, 6.31 MeV level indicating that they are high spin states. This is not only because high spin states are expected to occur at higher energy but also because the natural breakup of  $^{22}\text{Ne}$  by  $\alpha$  emission above 9.67 MeV and  $n$  emission above 10.37 MeV excitation makes highly excited low spin states difficult to observe via  $\gamma$  decay.

A summary of the results for these  $\gamma$ -emitting levels is given in Table III. The first column gives the initial level number while the second column shows the levels through which the initial level decays and for which correlations have been fitted. In each case a sequence of arrows shows a cascade through the levels indicated and a semi-colon separates a cascade of transitions from a parallel cascade. The unnormalized  $\chi^2$ 's are listed under the column headings for the assumed spins

0 to 8. In each case, a value of  $\chi^2$  is listed for each spin of the initial state that is allowed by the observed  $\gamma$  decay branches given in Table II. The final columns of Table III list the 0.1% confidence level of  $\chi^2$  for each case and also the number of degrees of freedom. These last quantities are not strictly the same for all fits in a given row since the number of multipole mixing ratios may vary by one depending on the assumed initial spin. For the sake of simplicity, this small variation in the significance level has been ignored. It will be seen that for many cases unique values of the spin of the initial state were not obtained.

Table IV lists the possible mixing ratios for all of the acceptable correlation fits shown in Table III which gave  $\chi^2$  below the 0.1% limit. The terms "quad" and "dipole" are used when the spins require a transition to be pure quadrupole or dipole, respectively. In principle, where more than one transition has been fitted simultaneously, the mixing ratios from different transitions are correlated. In practice it was found that the correlation was negligible.

## V. DISCUSSION

Table V summarizes the spins allowed for the  $^{22}\text{Ne}$  levels investigated here together with spin and parity information from earlier work. The

TABLE IV. Multipole mixing ratios for  $^{22}\text{Ne}$  transitions.

| Initial no. | Level spin | Final no. | Level spin | Mixing ratio                                    |
|-------------|------------|-----------|------------|---|
| 7           | 2          | 2         | 4          | Quad  |
|             | 3          |           |            | $0.44 \pm 0.16$                                 |
|             | 4          |           |            | $0.12 \pm 0.15(-1.0 \pm 0.2, -0.18 \pm 0.18)^a$ |
| 8           | 2          | 1         | 2          | $0.37 \pm 0.05$                                 |
|             | 2          | 2         | 4          | Quad  |
|             | 3          | 1         | 2          | $-0.16 \pm 0.03; >19, <-59$                     |
| 9           | 3          | 2         | 4          | $-0.00 \pm 0.10$                                |
|             | 1          | 1         | 2          | $-0.21 \pm 0.03$                                |
|             | 3          |           |            | $0.02 \pm 0.02$                                 |
| 10          | 1          | 1         | 2          | $-2.4^{+0.6}_{-1.3}; 0.7 \pm 0.1$               |
|             | 2          |           |            | $-0.03 \pm 0.06; -1.27^{+0.17}_{-0.23}$         |
|             | 3          |           |            | $-4.0^{+0.7}_{-1.0}$                            |
| 12          | 6          | 2         | 4          | Quad  |
| 16          | 1          | 0         | 0          | Dipole  |
|             |            | 1         | 2          | $5.3^{+6.4}_{-1.9}; -0.11 \pm 0.10$             |
|             |            | 3         | 2          | $0.07 \pm 0.3$                                  |
|             | 2          | 0         | 0          | Quad  |
|             |            | 1         | 2          | $>14, <-9; 0.5 \pm 0.1$                         |
|             |            | 3         | 2          | $-0.27 \pm 0.16$                                |
| 19          | 0          | 1         | 2          | Quad  |
|             | 1          |           |            | $0.06 \pm 0.17; 3.0^{+1.3}_{-0.7}$              |
|             | 2          |           |            | $>10, <-5$                                      |
|             | 3          |           |            | $>66, <-82$                                     |
| 20          | 3          | 2         | 4          | $1.2^{+0.3}_{-0.2}$                             |
|             | 4          |           |            | $-1.0^{+0.15}_{-0.21}; -0.01 \pm 0.09$          |
|             |            |           |            |   |
| 23          | 3          | 7         | 4          | $-2.9^{+0.4}_{-0.6}; -0.48 \pm 0.06$            |
|             | 5          | 7         | 4          | $0.18 \pm 0.03$                                 |
| 29          | 2          | 1         | 2          | $0.33 \pm 0.20$                                 |
|             |            | 2         | 4          | Quad  |
|             | 3          | 10        | 2          | $>1.0, <-250$                                   |
|             |            | 1         | 2          | $-0.09 \pm 0.09; 5.7^{+10}_{-2.2}$              |
|             |            | 2         | 4          | $+0.9 \pm 0.10; 3.7^{+2.7}_{-1.1}; >203, <-25$  |
|             |            | 10        | 2          | $>360, <-400$                                   |
|             | 4          | 1         | 2          | Quad  |
|             |            | 2         | 4          | $-4.1^{+1.1}_{-1.0}; 0.55 \pm 0.23$             |
|             |            | 10        | 2          | Quad  |
|             |            |           |            |   |
| 32          | 3          | 1         | 2          | $3.9 \pm 0.4; -0.02 \pm 0.02$                   |
|             |            | 2         | 4          | $-0.36 \pm 0.22, -0.25 \pm 0.15$                |
| 33          | 3          | 2         | 4          | $0.86 \pm 0.17$                                 |
|             | 4          |           |            | $-0.26 \pm 0.18$                                |
| 34          | 5          | 2         | 4          | $-0.03 \pm 0.04$                                |
|             |            |           |            | $0.17 \pm 0.14$                                 |
| 37          | 2          | 2         | 4          | Quad  |
|             |            | 3         | 2          | $0.07 \pm 0.07$                                 |
|             | 3          | 2         | 4          | $0.02 \pm 0.06; 5.7^{+3.6}_{-1.6}$              |
|             |            | 3         | 2          | $-4.2^{+1.0}_{-1.9}; -0.43 \pm 0.08$            |
|             | 4          | 2         | 4          | $0.64 \pm 0.14$                                 |
| 49          | 5          | 3         | 2          | Quad  |
|             |            | 2         | 4          | $0.01 \pm 0.03; 10.4^{+4.5}_{-2.4}$             |
|             |            |           |            |   |
| 55          | 4          | 12        | 6          | $0.06 \pm 0.07; 6.1^{+4.3}_{-1.8}$              |
|             |            |           |            | Quad  |
|             |            | 5         |            | $0.41 \pm 0.07; 1.9 \pm 0.3$                    |
|             |            | 6         |            | $0.22 \pm 0.09; -1.1 \pm 0.2$                   |
|             | 7          |           |            | $-0.37 \pm 0.04$                                |
| 56          | 5          |           |            | Quad  |
|             |            | 2         | 4          | $9.6^{+4.7}_{-2.4}; 0.02 \pm 0.04$              |
|             |            | 12        | 6          | $0.14 \pm 0.04; 4.1^{+0.9}_{-0.6}$              |

TABLE IV (Continued)

| Initial no. | Level spin | Final no. | Level spin | Mixing ratio                |
|-------------|------------|-----------|------------|-----------------------------|
| 57          | 5          | 2         | 4          | $0.05 \pm 0.04$             |
|             |            | 12        | 6          | $-0.10 \pm 0.05; >41, <-22$ |
| 58          | 6          | 12        | 6          | $-0.92 \pm 0.09$            |
|             | 8          |           |            | Quad                        |
| 59          | 6          | 12        | 6          | $0.01 \pm 0.08$             |
|             | 7          |           |            | $-0.46 \pm 0.04$            |
|             | 8          |           |            | Quad                        |
| 60          | 7          | 12        | 6          | $0.02 \pm 0.01$             |

<sup>a</sup> From the fitting of level 22, 23.

first reference quoted is the compilation of Endt and van der Leun<sup>18</sup> which includes early work such as the  $(\alpha, p\gamma)$  correlation measurements of Kutschera, Pelte, and Schrieder<sup>4</sup> and the inelastic  $\alpha$ -scattering work of Ollerhead *et al.*<sup>6</sup> Additional references in Table V are the  $^{20}\text{Ne}(t, p\gamma)^{22}\text{Ne}$  particle- $\gamma$  correlation work of Howard *et al.*,<sup>5</sup> the  $^{21}\text{Ne}(d, p)^{22}\text{Ne}$  and  $^{18}\text{O}(^7\text{Li}, t)^{22}\text{Ne}$  particle transfer experiments of Neogy *et al.*,<sup>19,20</sup> and the high resolution Ge(Li) detector  $\gamma$ -ray measurements of Davids *et al.*<sup>12</sup> and Fifield *et al.*<sup>15</sup> From Table V it can be seen that above 8 MeV there are one unique assignment of spin 3, four unique assignments of spin 5, and four assignments of spin 6 or greater. For the seven levels above 9 MeV the present work provides the only information available.

Table V indicates that there is disagreement

between spin information for the levels numbered 9, 16, 32, and 34. The 5.91 MeV level (9) had been assigned a spin of 2 by Kutschera *et al.*<sup>4</sup> using the same reaction as in the present experiment; however, detailed information on  $\chi^2$  for this and other possible spins was not given. Howard *et al.*<sup>5</sup> measuring proton- $\gamma$  correlations from the  $^{20}\text{Ne} + t$  reaction found spins of 1, 2, or 3 to be possible but pointed out that the mixing ratio required for spin 2 was in disagreement with Kutschera's value. In the present measurements only spins 1 and 3 are allowed in agreement with the conclusion of Howard *et al.* that the spin 2 assignment was not consistent with all of the data. Further, it should be pointed out that although spin 2 is quoted by Neogy *et al.*<sup>19</sup> they did not contribute any information on this level since it was only

TABLE V. Spin and parity information from this and other work.

| Level no. | $E_x$ (MeV) | Present    | Ref. 18                   | Ref. 5  | Ref. 12 | Ref. 19        | Preferred $J^\pi$                   |
|-----------|-------------|------------|---------------------------|---|---------|----------------|-------------------------------------|
| 7         | 5.52        | 2, 3, 4    | 4 <sup>+</sup>            |   |         | 4 <sup>+</sup> | 4 <sup>+</sup>                      |
| 8         | 5.64        | 2, 3       | 3 <sup>+</sup>            |   |         | 3 <sup>+</sup> | 3 <sup>+</sup>                      |
| 9         | 5.91        | 1, 3       | 2 <sup>+</sup>            | (1 <sup>-</sup> ), 2 <sup>+</sup> , (3 <sup>-</sup> ) |         |                | 3 <sup>-</sup>                      |
| 10        | 6.11        | 1, 2, 3    | Natural                   | 2 <sup>+</sup>  |         |                | 2 <sup>+</sup>                      |
| 12        | 6.31        | 6          | 6 <sup>+</sup>            |   |         |                | 6 <sup>+</sup>                      |
| 16        | 6.81        | 1, 2       | 2 <sup>+</sup>            | 1 <sup>-</sup>  |         | 2 <sup>+</sup> | 2 <sup>+</sup>                      |
| 19        | 7.04        | 0, 1, 2    | (1, 3) <sup>-</sup>       | 1 <sup>-</sup>  |         | 1 <sup>-</sup> | 1 <sup>-</sup>                      |
| 20        | 7.31        | 3, 4       | (0, 2, 4) <sup>+</sup>    |   | 3-5     |                | (3, 4) <sup>+</sup>                 |
| 23        | 7.41        | 3, 5       |                           |   | 3-5     |                | (3, 5) <sup>+</sup>                 |
| 29        | 7.70        | 2, 3, 4    | (1, 3) <sup>-</sup>       |   |         | 3 <sup>-</sup> | 3 <sup>-</sup>                      |
| 32        | 8.14        | 3          | (0, 2, 4) <sup>+</sup>    |   |         | 2 <sup>+</sup> |                                     |
| 33        | 8.35        | 3, 4       | Natural                   |   |         |                |                                     |
| 34        | 8.44        | 5          | (1, 2) <sup>+</sup>       |   |         |                |                                     |
| 37        | 8.72        | 2, 3, 4, 5 | (0, 1, 2, 3) <sup>-</sup> |   |         |                |                                     |
| 49        | 9.61        | 5          |                           |   |         |                | 5                                   |
| 55        | 10.41       | 6, 8       |                           |   |         |                | 6, 8                                |
| 56        | 10.64       | 5          |                           |   |         |                | 5                                   |
| 57        | 10.76       | 5          |                           |   |         |                | 5 <sup>-</sup>                      |
| 58        | 11.00       | 8          |                           |   |         |                | 8 <sup>+</sup>                      |
| 59        | 11.11       | 6, 7, 8    |                           |   |         |                | 6 <sup>-</sup> , 7 <sup>+</sup> , 8 |
| 60        | 11.48       | 7          |                           |   |         |                | 7                                   |

weakly excited. The work of Ollerhead *et al.*<sup>6</sup> shows that the 5.91 MeV state has natural parity, indicating either  $1^-$  or  $3^-$ . This implies that the decay of this state to the  $2^+$  first excited state should be predominantly dipole, especially as  $^{22}\text{Ne}$  is not self-conjugate and electric dipole transitions are not hindered by isospin selection rules. From Table IV it can be seen that only spin 3 has a zero mixing ratio, i.e., pure dipole, allowing the conclusion that the 5.91 MeV level is  $3^-$ . This is in agreement with the work of Howard *et al.*

The 6.81 MeV level (16) has conflicting spin assignments from information prior to the present work. The study of Neogy *et al.*<sup>19</sup> combined with the results of Ollerhead *et al.*,<sup>6</sup> who assigned natural parity to this state, results in a definite  $2^+$  assignment. Howard *et al.*<sup>5</sup> claim  $1^-$  but they could not resolve the level from its close neighbor at 6.84 MeV. The present work assigns spin 1 or 2, thus not resolving the problem directly. However, a  $1^-$  assignment would require a pure dipole transition between the 6.81 and 4.45 MeV levels whereas the correlation fit requires a large quadrupole admixture, the mixing ratio being  $0.7 \pm 0.3$ . It is concluded therefore that  $2^+$  is the most probable assignment to the 6.81 MeV level.

The spin assignments to levels 32 and 34 at 8.14 and 8.44 MeV are in disagreement with the values from the  $^{21}\text{Ne}(d,p)^{22}\text{Ne}$  reaction.<sup>19</sup> In addition the excitation energies of these levels show anomalous deviations from the energies of Ref. 18 (see Table I) indicating that the levels excited in the  $(\alpha,p)$  reaction may not be those seen in the  $(d,p)$  reaction.

The levels observed at 7.31 (20) and 7.41 (23) MeV also show energy anomalies. The situation with regard to the level at 7.31 MeV is confused. Levels at about this energy have been assigned  $0^+$  from the  $^{18}\text{O}(^7\text{Li},t)^{22}\text{Ne}$  reaction<sup>20</sup> and  $4^+$  from the  $^{20}\text{Ne}(t,p)^{22}\text{Ne}$  reaction.<sup>21</sup> Ollerhead *et al.*<sup>6</sup> have assigned natural parity to a level at this energy. The  $^{21}\text{Ne}(d,p)^{22}\text{Ne}$  reaction indicates an  $l=2$  transfer which, with natural parity, indicates  $(0,2,4)^+$  quoted by Endt and van der Leun.<sup>18</sup> Davids *et al.*<sup>12</sup> have assigned a spin of  $(3-5)^+$  to a level at 7.341 MeV, in complete contradiction with the  $\alpha$ -particle transfer work. This level was seen to decay by  $\gamma$  emission entirely to the 3.35 MeV  $4^+$  state. Davids's observations are in agreement with the properties of the 7.31 MeV state observed in the present experiment. It appears that there must be at least two close levels at this energy and that the level seen in the present work is the same as that seen by Davids *et al.*, limiting its spin to  $(3,4)^+$ .

The level at 7.41 MeV corresponds well with the level assigned  $(3-5)^+$  at 7.424 MeV by Davids *et al.*<sup>12</sup> The present results assign 3 or 5 with the same decay mode, entirely to the 5.52 MeV state.

It is noted that the accurate energy difference between the latter two levels determined by Davids *et al.* is 83 keV, while it is 93 keV from the present experiment. This discrepancy, in addition to the unusual decay mode of the 7.41 MeV level, raises the possibility that the 7.31 MeV level of this work is not the same as the 7.341 MeV state of Davids *et al.*

Six levels included in Table V lie above the  $^{22}\text{Ne}$  breakup thresholds for  $\alpha$  emission (9.67 MeV) and neutron emission (10.37 MeV). A consideration of the competition between  $\gamma$  emission and the two open particle channels allows us to eliminate certain assignments. For these levels, expressions and tabulations for single particle  $\gamma$  widths, reduced particle widths, and penetrabilities have been taken from the compilation of Marion and Young.<sup>22</sup>  $\alpha$  decay from these levels is to the  $0^+$  ground state of  $^{18}\text{O}$ , and so can occur only from natural parity  $^{22}\text{Ne}$  states. The 10.41 MeV state is barely above the neutron threshold; the Wigner limit for  $\alpha$  emission is 10 eV for  $l=4$ , while the  $E2$  radiation width is 3 meV. Allowing for a reasonable reduction of the  $\alpha$  width and enhancement of the  $E2$ , the  $4^+$  assignment to the 10.41 MeV state can be eliminated. A  $4^-$  assignment can also be eliminated, although it has no allowed  $\alpha$  decay, since the observed  $\gamma$  decay would be  $M2$  in competition with possible  $E1$  transitions to lower states which are not observed. Assignments of 5 and 7 are eliminated because the correlation analysis requires significant quadrupole amplitudes in the  $\gamma$  decay which would have to be  $M2$  in competition with  $E1$ . No other restriction can be applied to this level.

The 10.64 and 10.76 MeV levels have unique assignments of 5. The latter level has mixing ratios which within reasonable errors could be consistent with pure dipole radiation and so with negative parity. The former level is close to this situation. The  $\alpha$  and neutron widths from these levels for  $l=5$  and 3, respectively, are sufficiently small to allow such a possibility.

The levels at 11.00 MeV and above have sufficient energy to decay by neutron emission to both the ground ( $\frac{3}{2}^+$ ) and first excited ( $\frac{5}{2}^+$ ) 350 keV states in  $^{21}\text{Ne}$ . It appears that the 11.00 MeV state cannot be  $6^-$  because of the large implied  $M2$ ;  $6^+$  seems unlikely also, because the neutron width (70 eV) is much larger than the implied  $E2$  width (4 meV). This leaves an assignment of 8 for the 11.00 MeV level. The 11.11 MeV level is consistent with  $6^-$ ,  $7^+$ ,  $8^+$ , or  $8^-$  while the 11.48 MeV level is consistent with  $7^+$  or  $7^-$ .

It is to be expected that  $^{22}\text{Ne}$  levels can be incorporated into a rotational-like band structure similar to those found in  $^{20}\text{Ne}$  and  $^{24}\text{Mg}$ . In  $^{22}\text{Ne}$  the classification is more speculative than in the

neighboring nuclei since it is based almost solely on level energies and spin-parity assignments. In the self-conjugate neighbors, isospin selection rules operate to inhibit cross-band  $E1$  transitions so that the in-band  $E2$  radiative transitions are easily observed. Since many of the lifetimes are within the range of experimental methods, such measurements are sensitive indicators of band structure. In  $^{22}\text{Ne}$  however, the  $E1$  transitions tend to dominate the decay modes making  $E2$  branches very weak and lifetimes very short. It is nevertheless instructive to try to group some of the known  $^{22}\text{Ne}$  levels into bands, in part as an incentive for further experimental work.

An extensive discussion of the classification of  $^{22}\text{Ne}$  in terms of  $\text{SU}(3)$  has been given by Scholz *et al.*<sup>20</sup> For levels above 6.5 MeV their discussion was based on the results of the  $^{21}\text{Ne}(d,p)$  and  $^{18}\text{O}(^7\text{Li},t)$  reactions. It is not always possible to be sure that the levels they discuss correspond to levels seen in the present work. However, their discussion will be the basis for the present interpretation of the  $^{22}\text{Ne}$  levels which is shown in Fig. 8.

The leading  $\text{SU}(3)$  representation  $(\lambda\mu) = (82)$  gives rise to a ground state band whose  $0^+$ ,  $2^+$ ,  $4^+$ , and

$6^+$  members have long been known as the ground, 1.28, 3.34, and 6.31 MeV levels. The present work assigns a most likely  $8^+$  member of the band at 11.00 MeV. Reanalysis of the data reported in Ref. 9 indicates that the 10.41 MeV level is strictly within the 0.1% limit for spin 8; however, spin 6 is much more probable for this level. Spin 6 for the 11.00 MeV level is unlikely as seen earlier so that the 11.00 MeV state is the most likely lowest spin 8 state. In a truncated shell model calculation, Arima, Sakakura, and Sebe<sup>8</sup> find the lowest  $8^+$  level at 11.27, in close agreement with experiment.

The same  $\text{SU}(3)$  representation also gives rise to a  $K=2^+$  band. From the known levels, it is possible to suggest a band that starts with the  $2^+$  level at 4.47 MeV and includes the  $3^+$  5.64,  $(4)^+$  6.35, and the  $5^+$  7.41 MeV levels (numbered 3, 8, 13, and 23). A  $K=1^+$  band can be built on the  $1^+$  5.33 MeV level by including the  $2^+$  6.81,  $3^+$  7.31,  $(4)^+$  8.35, and  $5^{(+)}$  9.61 MeV levels. If it turns out that the 11.11 MeV level is  $6^+$ , requiring the neutron width to be very small, it would be a possible  $6^+$  member of this band. There is no other indication of the origin of the 11.11 MeV high spin state although Arima *et al.*<sup>8</sup> predict a second  $8^+$  state at about 12

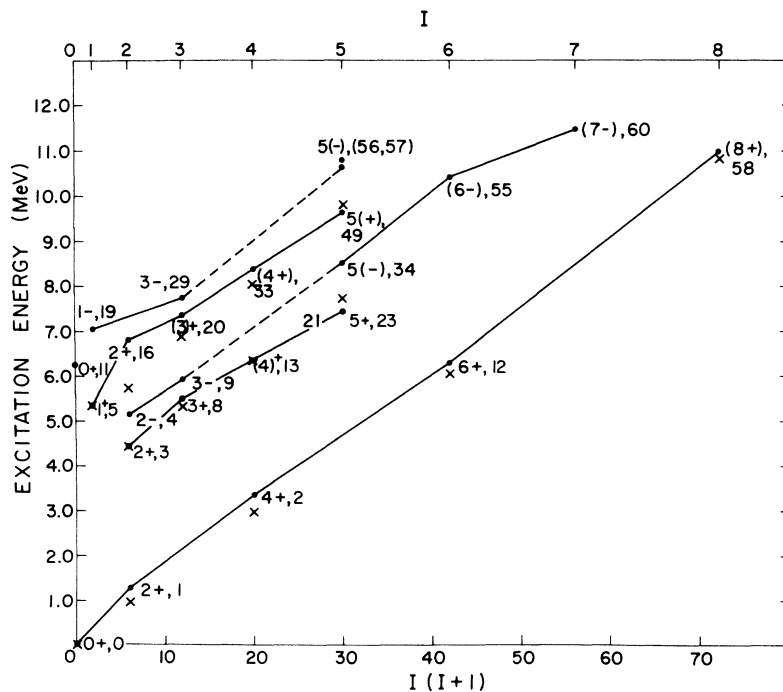


FIG. 8. Proposed rotational level scheme for  $^{22}\text{Ne}$ . The spins and parities are consistent with all known data, but are bracketed if the quantity has not been uniquely assigned. The level numbers used throughout this article are also indicated for each level. Dotted lines indicate no candidates for intermediate band members. The crosses are the predictions of Johnstone and Castel for the lowest  $K=0^+$ ,  $1^+$ , and  $2^+$  bands. The lowest member of each band is normalized to the experimental energy (see text).

MeV. A  $K=1^+$  band results from the (63) representation. Scholz *et al.*<sup>20</sup> pointed out that a  $1^+$  band would also arise from the (71) representation and that the bandhead of this could be the 6.86 MeV  $1^+$  level. No extensions of this band have been found.

Some candidates for a  $K=2^-$  band resulting from the (84) representation are indicated in Fig. 8. These include the  $2^-$  5.14,  $3^-$  5.91,  $5^{(-)}$  8.44,  $(6^-)$  10.41, and  $(7^-)$  11.48 MeV levels. Note that we have found no suitable candidate for a  $4^-$  level which should be in the neighborhood of level 21.

Scholz *et al.* suggested that the  $1^-$  7.06 and  $3^-$  7.73 MeV levels belong to the (11,1) representation, the only source of a  $K=1^-$  band. They noted that no evidence exists for a  $2^-$  member; none has been found in this experiment. A  $5^-$  candidate for this band is one of the two spin 5 levels at 10.64 and 10.75 MeV (levels 56 and 57). No  $4^-$

member has been found.

Finally, the band mixed projected Hartree-Fock calculations of Johnstone and Castel<sup>23</sup> have been extended to higher energies<sup>24</sup> and their results for the lowest  $K=0^+$ ,  $1^+$ , and  $2^+$  bands are included in Fig. 8. The Kuo interaction used in these calculations is known to give the spacings within a band quite well but to make errors in the prediction of bandhead energies; consequently we have normalized the lowest member of each band to the experimental value ( $K=0^+$  to level 0,  $K=1^+$  to level 5, and  $K=2^+$  to level 3). Except for level 16, the  $2^+$  member of the  $K=1^+$  band, reasonable agreement is obtained between experimental and calculated bands.

The authors wish to thank Miss A. R. Rutledge for her patience in handling the data over an extended period of time.

\*Permanent address: Physics Department, Weizman Institute of Science, Rehovot, Israel.

<sup>1</sup>J. W. Olness, W. R. Harris, P. Paul, and E. K. Warburton, *Phys. Rev. C* **1**, 958 (1970) and references contained therein.

<sup>2</sup>H. Grawe, K. Holzer, K. Kändler, and A. A. Pilt, *Nucl. Phys. A* **237**, 18 (1975).

<sup>3</sup>A. E. Litherland and A. J. Ferguson, *Can. J. Phys.* **39**, 788 (1961).

<sup>4</sup>W. Kutschera, D. Pelte, and G. Schrieder, *Nucl. Phys. A* **111**, 529 (1968).

<sup>5</sup>A. J. Howard, R. G. Hirko, D. A. Bromley, K. Bethge, and J. W. Olness, *Nuovo Cimento* **11A**, 575 (1972).

<sup>6</sup>R. W. Ollerhead, G. F. R. Allen, A. M. Baxter, B. W. J. Gillespie, and J. A. Kuehner, *Can. J. Phys.* **49**, 594 (1971).

<sup>7</sup>G. C. Ball, G. J. Costa, W. G. Davies, and J. S. Forster, Chalk River Reports Nos. AECL-4428 and AECL-4595 (unpublished).

<sup>8</sup>A. Arima, M. Sakakura, and T. Sebe, *Nucl. Phys. A* **170**, 273 (1971).

<sup>9</sup>C. Broude, W. G. Davies, and J. S. Forster, *Phys. Rev. Lett.* **25**, 944 (1970).

<sup>10</sup>P. D. Stevens-Guille, Atomic Energy of Canada Ltd., Report No. CRNL-31, 1967 (unpublished).

<sup>11</sup>W. W. Black, *Nucl. Instrum. Methods* **71**, 317 (1969).

<sup>12</sup>C. N. Davids, D. R. Goosman, D. E. Alburger, A. Gall-

mann, G. Guillaume, D. H. Wilkinson, and W. A. Lanford, *Phys. Rev. C* **9**, 216 (1974).

<sup>13</sup>W. G. Davies and J. S. Forster (private communication).

<sup>14</sup>A. J. Ferguson, in *Proceedings of the Symposium on Applications of Computers to Nuclear and Radio Chemistry*, Gatlinburg, Tennessee 1962 (unpublished), Report No. NAS-NS-3107.

<sup>15</sup>L. K. Fifield, R. W. Zurmühle, and D. P. Balamuth, *Phys. Rev. C* **10**, 1785 (1974).

<sup>16</sup>E. M. L. Beale, *J. Roy. Stat. Soc. B* **17**, 173 (1955).

<sup>17</sup>A. J. Ferguson, *Angular Correlation Methods in Gamma-ray Spectroscopy* (North-Holland, Amsterdam, 1965).

<sup>18</sup>P. M. Endt and C. van der Leun, *Nucl. Phys. A* **214**, 1 (1973).

<sup>19</sup>P. Neogy, R. Middleton, and W. Scholz, *Phys. Rev. C* **6**, 885 (1972).

<sup>20</sup>W. Scholz, P. Neogy, K. Bethge, and R. Middleton, *Phys. Rev. C* **6**, 893 (1972).

<sup>21</sup>E. R. Flynn, O. Hansen, and O. Nathan, *Nucl. Phys. A* **228**, 189 (1974).

<sup>22</sup>J. B. Marion and F. C. Young, *Nuclear Reaction Analysis* (North-Holland, Amsterdam, 1968).

<sup>23</sup>I. P. Johnstone and B. Castel, *Lett. Nuovo Cimento* **3**, 307 (1970).

<sup>24</sup>I. P. Johnstone (private communication).